Conductivity studies of polyaniline doped with CSA

Conductivity studies of polyaniline doped with CSA

E R Holland, S J Pomfret†, P N Adams and A P Monkman

Organic Electroactive Materials Group, Physics Department, Science Site, South Road, Durham DH1 3LE, UK

Abstract. Polyaniline films prepared via the camphorsulphonic acid (CSA)m-cresol solution processing route have been synthesized with doping levels in the range of 10–90%. The electrical conductivity of these films has been measured as a function of temperature between 10 and 300 K. At a doping level of 30% the onset of metallic transport is observed, and at 60% the films are found to exhibit metallic transport down to 135 K, and have a maximum room-temperature conductivity of 300 ± 30 S cm^{-1}. The results are modelled in terms of a heterogeneous model of fluctuation induced tunnelling (FIT) and metallic transport.

1. Introduction

Polyaniline (PANi) is continuing to receive considerable interest in the field of conducting polymers. The electrically conductive emeraldine salt form of polyaniline is air stable and cheap to produce in large quantities [1], giving rise to many suggestions for possible applications of the material [2].

Until recently the polymer has only been processable in the emeraldine base (EB) form, requiring post-doping with a protonic acid to give the required emeraldine salt (ES). This is not a totally satisfactory processing route as it is difficult to achieve totally homogeneous doping in such dense films [3].

Cao *et al* have recently overcome the problem of processing ES by the discovery of acid solution processing routes [4]. The routes use two specific functional acids, camphor sulphonic acid (CSA) and dodecylbenzene sulphonic acid (DBSA) in organic solvents.

One such system has proven to be of considerable interest. This is PANi:CSA in m-cresol. Recent work has shown that this material possesses metallic characteristics at high temperatures, i.e. a positive temperature coefficient of resistivity [5, 6]. This behaviour has been interpreted in two ways: firstly as indicating that the PANi:CSA is a disordered metal near the metal–insulator boundary [5], and alternatively as being a modified Drude metal—with the modifications being due to localization within the system [6]. It is useful, at this point, to outline what is meant by a disordered metal near the metal–insulator boundary.

When there is a finite density of states at the Fermi energy (E_F) a system is usually considered to be a metal. If however, these states are localized, there remains a finite density of states at E_F but the system is not metallic—it is a Fermi glass. In a Fermi glass the conductivity is thermally activated. If E_F is located in localized states *just below* the energy where the states become delocalized (the mobility edge), then at higher temperatures the thermal energy will be sufficient to activate carriers to the band of delocalized states.

† E-mail: S.J.Pomfret@durham.ac.uk

Conductivity is then expected to follow a power law temperature dependence. At lower temperatures the carriers are restricted to localized states, and the conductivity will be governed by some hopping or tunnelling mechanism. Such a system is described as a metal close to the metal–insulator boundary.

Previous studies of the conductivity of ES have shown that the maximum conductivity is achieved upon protonation of 50% of the nitrogen sites [7, 8], which is commonly referred to as 50% doping in the literature. Subsequent to this work most studies into the electrically conductive nature of ES have concentrated on 50% doped samples. This paper reports investigations of the electrically conductive nature of PANi:CSA films with doping levels ranging from 10–90%. The conductivity of the samples has been measured as a function of temperature in the range 10–300 K. Definite trends in the temperature dependence of the conductivity have been recorded, with the more highly doped samples showing the previously observed positive temperature coefficient of resistivity indicative of metallic behaviour.

2. Experimental details

The synthesis route for the PANi has been described elsewhere [9]. The free-standing PANi:CSA films were prepared in the following manner. Appropriate amounts of PANi and CSA were mixed in a mortar and pestle. These powder mixtures were then dissolved in *m*-cresol so as to give 1.6% by weight solutions. These solutions were then homogenized using an Ultra-Turrax T25 homogenizer for approximately 15 min, and poured onto polished silicon wafers. The films were dried at 60 °C under a dynamic vacuum for 20 h. The films could then be peeled off from the substrate to give high-quality free-standing samples, with thicknesses varying between 10 and 90 μm depending upon how much solution had been used to coat the wafer.

It is assumed that all the CSA protonates nitrogen sites in PANi and that errors in doping levels due to errors in weighing out the materials are less than 1%. However, for any doping level there is a larger ($\sim$ 10%) variation in the conductivity measurements between films. This has been noted previously by other groups [10], and is attributed to two main factors. Firstly, subtle changes in the morphology of the films arising from factors such as the variation of powder concentration in solution or the rate of evaporation of the solvent during the drying process may cause variations in the conductivity. Secondly, there will be errors associated with the measurement of the dimensions of the samples used in the conductivity measurements: width, thickness, and distance between contact points for the voltage measurement. These errors only affect the absolute values of conductivity, hence any trends shown in a temperature versus conductivity data set are not affected. In an effort to reduce these errors at least two samples of each doping level (apart from 10 and 20%) were measured. The 10 and 20% doped films were relatively brittle, making temperature dependent conductivity measurements difficult. The room-temperature conductivities of several of these samples were measured, however, and found to be in good agreement with the results shown here.

The conductivity of the samples was measured using the 'four-in-line' technique. For each film a section with dimensions about 5 mm by 20 mm was cut out and four parallel strips of gold evaporated onto one surface. The gold was used to ensure good electrical contacts during the experiment. The samples were placed in the specially constructed head of a Leybold closed loop helium cryostat, with pressure contacts to the four gold strips on the sample. Before cooling, the samples were left under dynamic vacuum for at least 5 h to ensure that all moisture and excess solvent had been removed; this resulted in the

conductivity falling by approximately 15%.

Conductivity measurements were then made between 10 and 300 K at 5 K intervals. For the less conductive samples the applied current was reduced from 1 mA to 100 μA so as to ensure that heating effects remained negligible.

3. Results and discussion

Figure 1(a) shows the plots of conductivity versus temperature for the films with doping levels between 10 and 60%, with figure 1(b) showing similar data for the films doped from 60 to 90%. It is clear that as the level of protonation is increased from 10 to 60% the conductivity increases rapidly. At 10 K the 60% doped sample is five orders of magnitude more conductive than the 10% doped sample. Also, the conductivity becomes a weaker function of temperature in the more heavily protonated films. The normalized conductivity, $\sigma(T)/\sigma(300\ \text{K})$, for each data set is shown in figure 2, and allows the trend in conductivity of each sample with temperature to be compared more easily.

At the two lowest levels of protonation (10 and 20%) the conductivity rises monotonically as temperature is increased. Additionally, the rate of increase of $\sigma(T)$ increases with temperature. When the protonation level reaches 30% and above the data reveal a very different behaviour. At low temperatures, conductivity increases as temperature rises, but at higher temperatures this rate of increase decreases. Moreover, each data set in the 30–90% doping range possesses a characteristic maximum in $\sigma(T)$ somewhere in the measured range. In table 1 typical peak positions and their accompanying conductivity values are presented. For each case, at temperatures above that at which the peak occurs, the conductivity decreases slowly with increasing temperature i.e. the electrical conductivity has a negative temperature coefficient. In figure 3 the data for the 50% doped sample are presented on a linear scale to reveal in detail the temperature dependence of the conductivity of highly conductive PANi:CSA.

Table 1. Temperature values at which the conductivity maxima occur in PANi:CSA.

| Protonation (%)	Peak conductivity (S cm^{-1})	Peak temperature (K)	$\sigma(10\ \text{K})/\sigma(300\ \text{K})$
30	90	270	0.13
40	130	225	0.44
50	178	190	0.67
60	268	135	0.94
70	184	184	0.75
90	121	185	0.71

It is widely accepted that the density of charge carriers within samples of conductive polyaniline is approximately equal to the density of protonated chain sites, up to a protonation level of 50%. If it is assumed that all the CSA dopant added to the polymer causes protonation above 50%, and that this increase in protonation causes an increase in charge carriers even where the theoretical 50% level is exceeded, it is possible to estimate the charge carrier density in samples prepared. Furthermore, using the general expression for electrical conductivity

$$\sigma = ne\mu$$
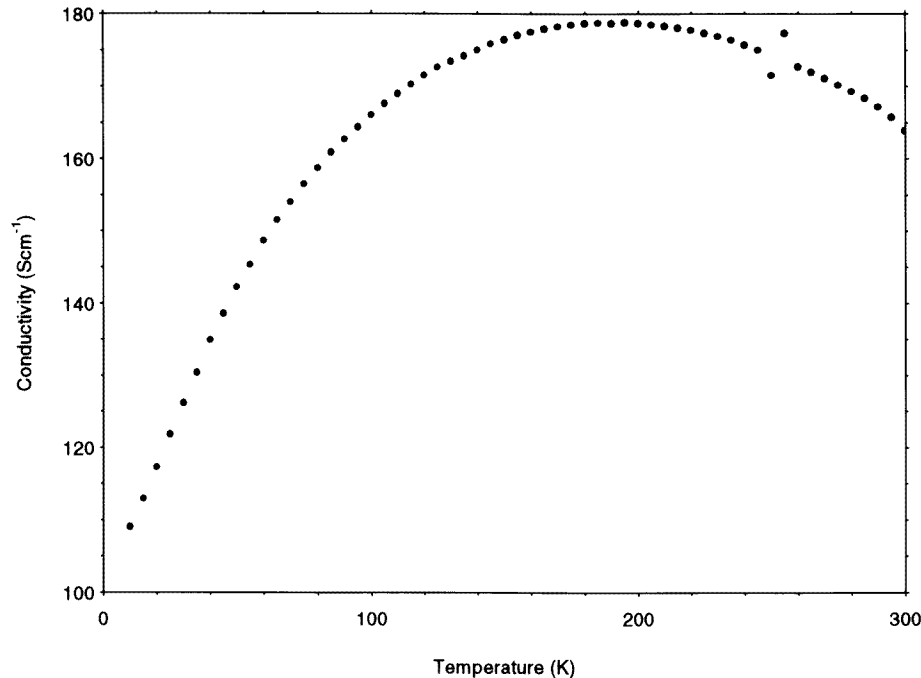
it is possible to make an estimate of the charge carrier mobility, μ, where n is the carrier

(*a*)

(*b*)
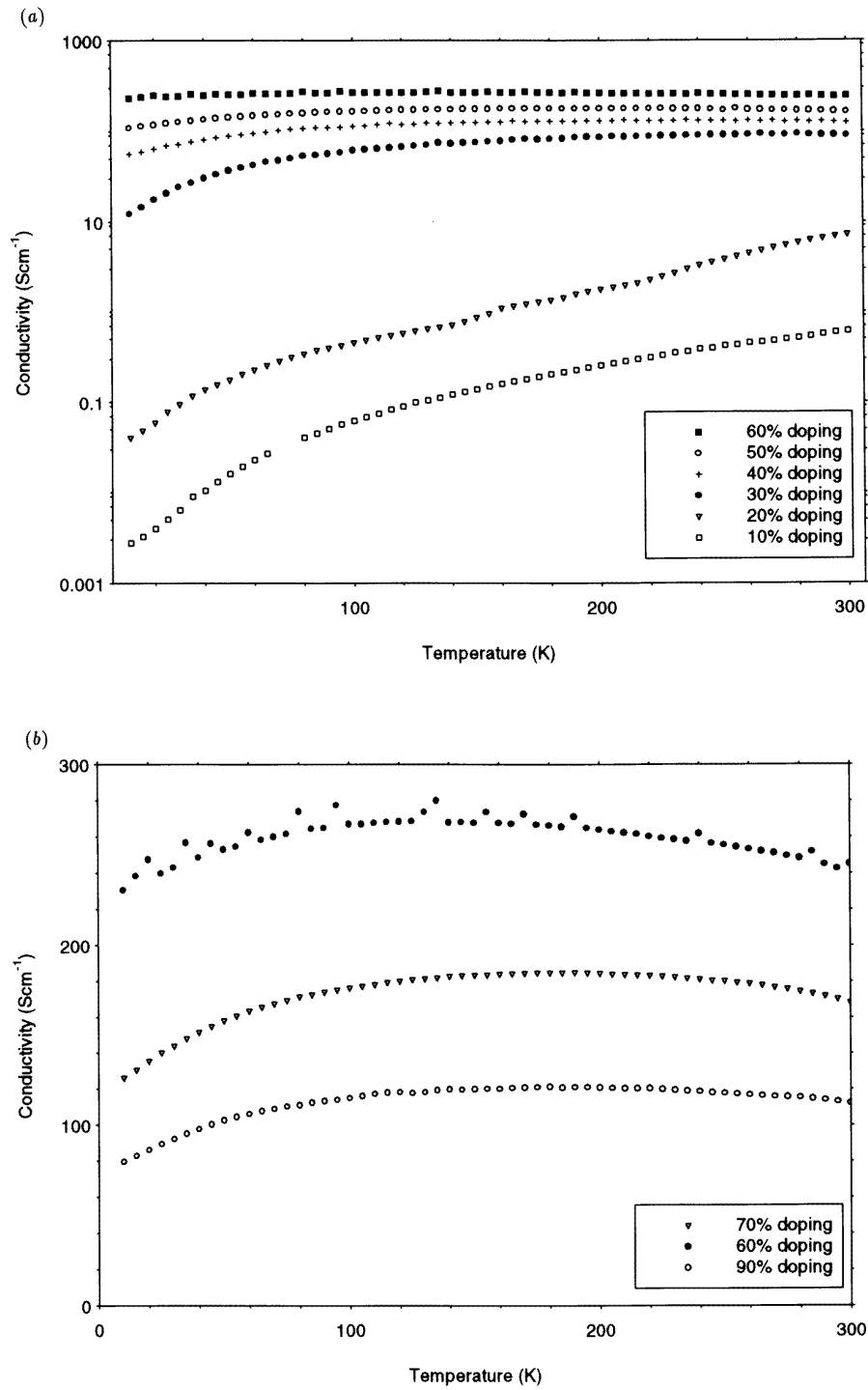
Figure 1. Conductivity as a function of temperature for films of various doping levels: (*a*) 10–60%; (*b*) 60–90%.

(*a*)

(*b*)
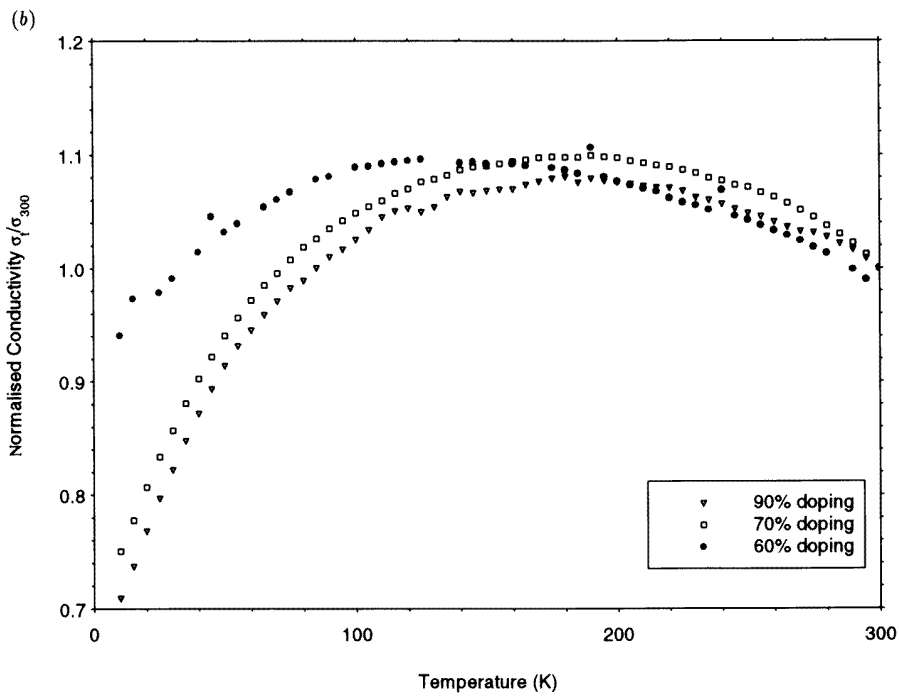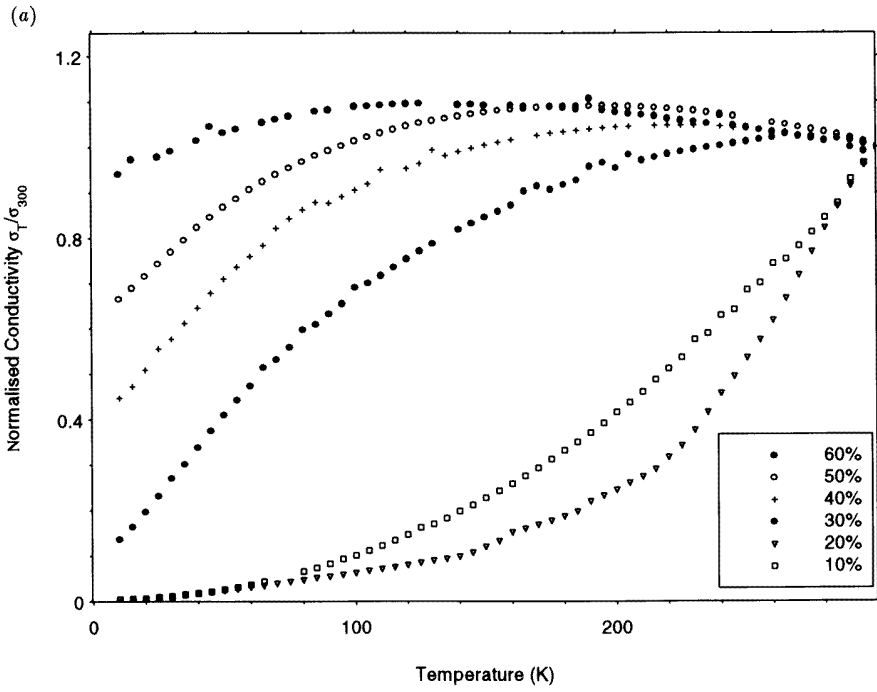
Figure 2. Normalized conductivity $(\sigma(T)/\sigma(300 \text{ K}))$ as a function of temperature for films of various doping levels: (*a*) 10–60%; (*b*) 60–90%.

Figure 3. A linear plot of conductivity as a function of temperature for a 50% doped film.

density and e is the charge on an electron. The results of these calculations are shown graphically in figure 4. The reduction of mobility at the higher doping levels (90%) may well be due to a break-down of the previous assumption.

From these results it would appear that there are two distinct regimes of charge transport in this material according to the level of protonation to which it is prepared. Samples prepared at 10 and 20% protonation, the two lowest doping levels, display an electrical conductivity which is a strong function of temperature, suggestive of charge carriers dependent upon some form of thermal activation. The variable-range hopping mechanism (VRH), in one or two dimensions, has been used to describe the charge transport observed in PANi from previous studies [11–13]. However, none of the data in figure 2(*a*) are characteristic of transport by VRH. At temperatures above 100 K the 10 and 20% samples can be described by the fluctuation induced tunnelling (FIT) model, which has the form

$$\sigma = \sigma_0 \exp\left[\frac{-T_1}{T + T_0}\right]$$

where T_1 depends upon the average potential barrier height and T_0 represents the temperature for which the thermal fluctuations produce a significant contribution to the tunnelling current compared with the temperature independent elastic tunnelling. At lower temperatures, however, the fit to these data based upon the form of this equation deviates significantly from the measured values.

A very different trend is revealed by the samples prepared with protonation levels in the range 30–90%. At low temperatures the conductivity still displays an activated behaviour. As the level of protonation is increased from 30% the decrease in the conductivity at the
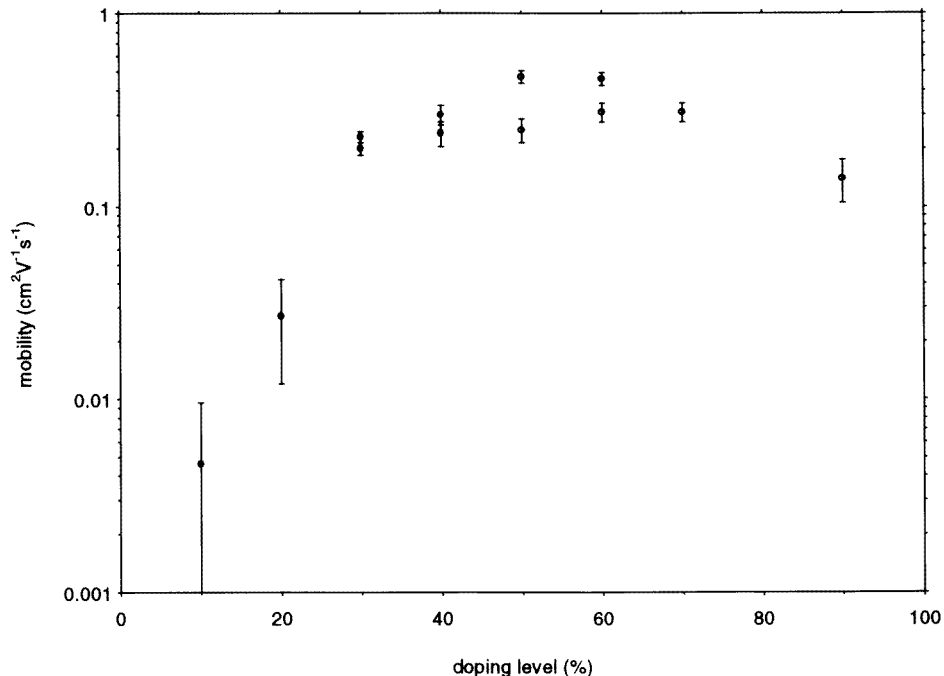
Figure 4. A plot of the charge carrier mobility (at room temperature) as a function of doping level.

lowest temperatures is much reduced, as illustrated by the values of $\sigma(T)/\sigma(300\ \text{K})$ in each case.

The results presented here suggest that the metallic behaviour extends to the lowest temperatures with the 60% protonated film, and that this doping level also results in the highest electrical conductivity. From figure 2, it is also evident that the reduction of conductivity at low temperatures is the least pronounced for the 60% doped films. This evidence implies that doping above the 50% level is capable of driving the PANi:CSA system far closer to the true metallic behaviour than observed in previous studies. Two explanations are suggested for why this may occur.

(i) Samples prepared with 50% doping do not react completely with the CSA added to the polymer. An excess of $10(\pm 5)\%$ acid is required to protonate all the imine sites on the polymer chain.

(ii) Protonation of more than 50% of the nitrogen sites generates more conduction band states and allows a higher charge carrier density within the material, up to a maximum at 60%.

From the results it is evident that PANi:CSA is an example of a conductor close to the metal–insulator boundary. For samples doped to 30% and above there is a transition in the nature of charge transport from hopping/tunnelling due to localization of carriers on some scale, to partial 'metallic' diffusion transport. The exact mechanism by which this transition occurs is unclear, but two explanations are suggested.

In the first picture, it is assumed that in the doping process protonation occurs completely at random, resulting in a homogeneous distribution over the available chain sites. At

low concentrations the conduction band states formed at protonated sites would be widely separated and the interaction between neighbouring sites limited. Consequently, charge carriers would be localized and thus conduction by thermally activated hopping, VRH, would be expected. In this case, as the doping level is increased, the average separation between conduction band states would decrease. Since this would have the effect of increasing both the charge carrier density and the strength of interaction between carrier states, an increase in conductivity and carrier mobility would be expected. At the highest doping levels, the high spatial density of doped sites may result in the formation of a conduction band containing both localized and diffuse electronic states, separated at some energy by a mobility edge. According to Larkin and Khmel'nitskii [14], in a system such as this where the Fermi level resides in the region of localized states but is close to the mobility edge, the conductivity at low temperatures follows a power law dependence upon temperature, i.e.

$$\sigma(T) \propto T^{1/\eta}$$

where $1 < \eta < 3$. At high temperatures, where the majority of charge transport is by carriers thermally excited to the band of delocalized states, conduction could be limited by phonon scattering giving rise to the negative temperature coefficient of conductivity observed by experiment.

This first theory provides a useful way to describe the behaviour of the highly conductive samples of PANi:CSA, i.e. those with 30% doping and above. However, the prediction of VRH transport at low doping levels is not supported by the experimental evidence presented previously.

The second theory which might account for the evolution of the conductive properties of PANi:CSA is that the doping process is not homogeneous on all scales. Protonation may occur in such a way that favours repeated doping of polymer chains or conglomeration of doped chains rather than an unbiased distribution, such that metallic islands are present when the material is cast as a solid film. As the level of doping is increased in this system, the number and/or size of metallic islands would be expected to increase. Hence an increase in the conductivity would occur due to three factors: the increased 'metallic' content of the sample, a reduction in the tunnelling/hopping distance between metallic regions, and the increased charge carrier density. At some threshold level of doping, significant overlap of metallic islands could permit a large fraction of charge transport via percolation. This would allow the charge transport within the metallic regions, rather than the tunnelling process, to become apparent in the properties of the bulk material.

Perhaps the most important feature of highly doped PANi:CSA is that the dc electrical conductivity is capable of displaying a negative temperature coefficient over a significant portion of the temperature range, e.g. above 135 K in the case of 60% doped samples. This provides direct evidence for charge transport mechanisms similar to those in crystalline metals. In this study, the onset and progression of this 'metallic' nature has been observed through measurements made on PANi samples with different doping levels up to and above the theoretical maximum of 50%. The origin of this character is now discussed in more detail.

The stark change in the behaviour of the conductivity between 20 and 30% doping suggests that there is a threshold within this range that marks the boundary between two charge transport regimes. At 30% doping, PANi:CSA is just able to display a metallic signature above a peak in conductivity at 270 K even though the conductivity (approximately 90 S cm^{-1}) is much lower than that of a typical metal. It is interesting to note, however, that the transition to pseudo-metallic behaviour occurs where samples have a conductivity of similar magnitude to that of the minimum metallic conductivity criterion [15]. This

describes a minimum value of conductivity which a disordered conductor can have before diffuse conduction band electronic states become localized and metallic charge transport can no longer be supported, and is in the range 100–300 S cm^{-1}. As the doping level is raised above 30% the metallic character becomes more evident: the peak conductivities occur at progressively lower temperatures, and thus the metallic behaviour is displayed over a larger range of temperature.

Previous x-ray analyses have shown that there is a significant degree of crystallinity in PANi:CSA [16–18]. In these crystalline regions of the polymer a precise phase order exists between adjacent polymer chains and this is expected to allow coherent electrical carrier transport along *and* between individual chains, i.e. the system has a regular polaron lattice structure. This means that carrier delocalization can occur in more than one dimension, on a scale larger than the average interchain separation. Therefore, the mean free path is limited not by scattering at interchain transfer events but by phonon scattering due to thermal motion of the crystal lattice, or by molecular vibrational modes. The properties of the crystalline regions could therefore account for the 'metallic' trends observed in the conductivity of PANi:CSA.

Further x-ray analysis is at present being undertaken to determine the physical structure of PANi:CSA films with various levels of doping [19]. Preliminary results suggests that there is a link between the type of crystal structure of the material and the level of CSA doping. The degree of conductivity appears to differ between the different crystal structures. If this is the case, then changing the level of doping will affect the conductivity not only by the two previouly described processes of changing the carrier concentration and altering the size of crystalline ('metallic') fraction, but also by changing the structure of the crystal phase.

Macroscopic charge transport within highly doped PANi-CSA is, however, not characteristic of that within a metal, and even in the case of the most highly conductive samples the conductivity decreases with decreasing temperature. It would therefore appear that there are at least two charge transport mechanisms that contribute to the properties of the bulk material. These must include a temperature activated process which results in the drop in conductivity seen in all cases at low temperatures. Secondly, at high temperatures the effects of a temperature dependent scattering process (phonon scattering) become apparent. This suggests that there is some transport by 'metallic' diffusion. The balance between these two mechanisms in any particular sample appears to depend upon the level of doping.

It is feasible therefore to view PANi:CSA as a composite material and invoke a heterogeneous conductor model. In this case it is proposed that there are two charge transport mechanisms at large in the polymer. These are metallic diffusion within the crystalline regions and temperature activated transport in the disordered or poorly doped regions.

Using this assumption it is possible to model the electrical conductivity for samples doped in the range 30–90%. The simplest approach is to consider the way in which each region of the sample contributes to the total resistivity of the bulk material. For the 'metallic' regions at temperatures above 10 K phonon scattering gives rise to an approximately linear increase in resistivity with temperature. For the disordered regions it is more difficult to justify the choice of any one mechanism. Having tried various models, the best fits have been achieved using the fluctuation induced tunnelling (FIT) model. The resistivity of the heterogeneous material is simply the sum of the individual resistivities due to each mechanism:

$$\rho = AT + B[\exp(-T_0/(T_1 + T))]^{-1}$$
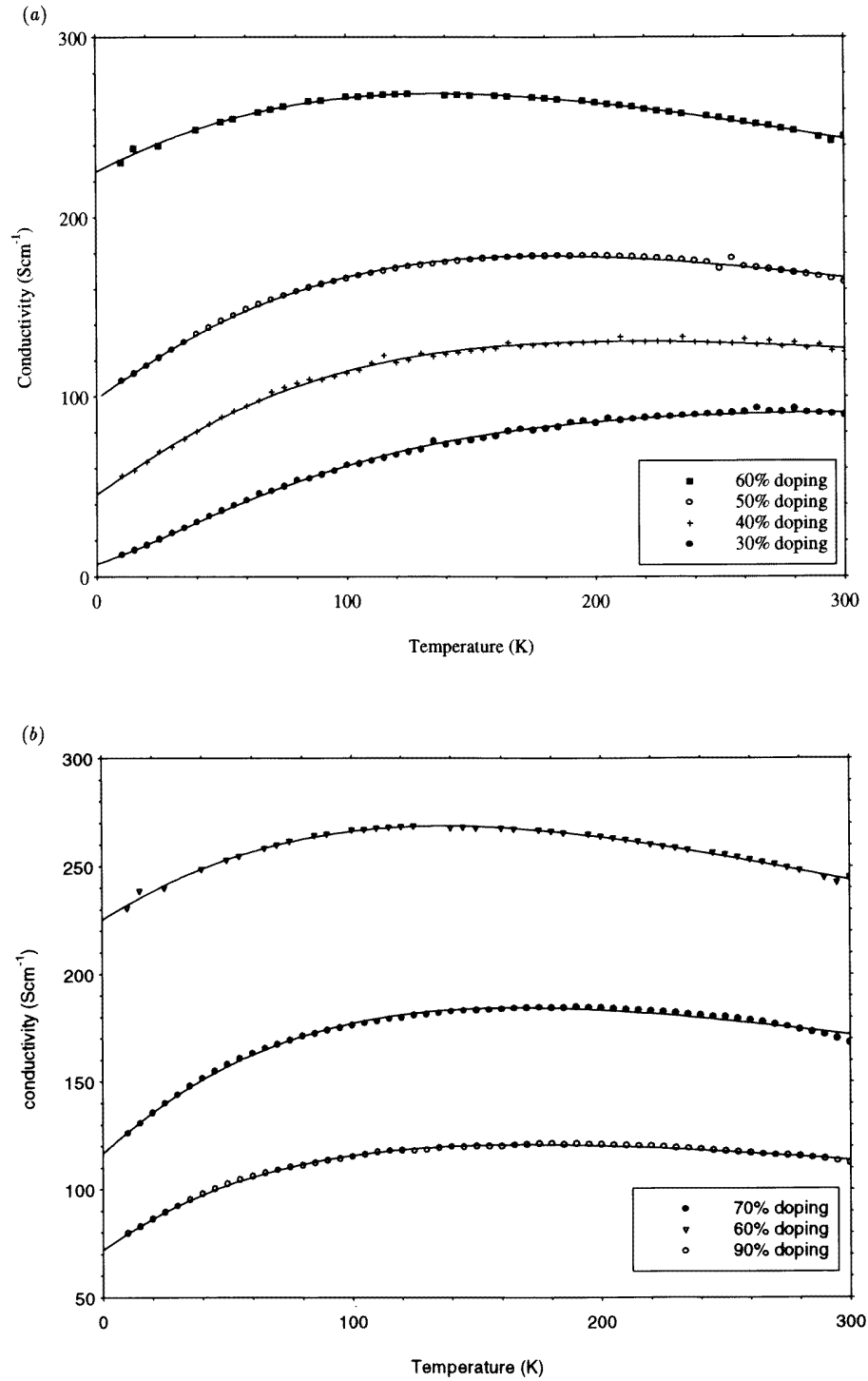
Figure 5. Fits for the heterogeneous model (explained in the text) with the conductivity data for films of various doping levels: (*a*) 10–60%; (*b*) 60–90%.

where A and B are fitting parameters and T_0 and T_1 are the characteristic temperatures in the FIT model as described previously. This expression has been used to generate curves that are a close fit to the conductivity data (see figure 5). The parameters for each curve are presented in table 2.

Table 2. Parameter values for the curve fits to the conductivity data for highly doped PANi:CSA.

Sample (% CSA)	A (Ω cm K^{-1})	B (Ω cm)	T_0 (K)	T_1 (K)
30	1.12×10^{-5}	4.49×10^{-3}	188	54
40	1.06×10^{-5}	2.93×10^{-3}	186	92
50	1.01×10^{-5}	1.48×10^{-3}	332	172
60	6.62×10^{-6}	9.31×10^{-4}	519	332
70	8.10×10^{-6}	2.22×10^{-3}	181	134
90	1.07×10^{-5}	4.10×10^{-3}	122	100

Although it is impossible to prove that charge transport really is governed by the particular mechanisms chosen for this heterogeneous model, the combination of FIT with phonon scattering provided far superior fits to other models, e.g. an expression with a phonon scattering term and a temperature activated term modelled on VRH, or a power law. To some extent, therefore, PANi:CSA appears to provide an example of a heterogeneous material in which there are crystalline, 'metallic' regions separated by disordered regions through which charge transport is via a tunnelling process.

4. Conclusions

PANi:CSA samples have been prepared with doping levels in the range 10–90%. The conductivity of these films has been measured as a function of temperature in the range 10–300 K. It has been shown that there are two distinct regimes of conductive behaviour. Below 30% doping the films have very low conductivity that fits a fluctuation induced tunnelling model above 100 K. At doping levels of 30% and above the films start to show metallic behaviour above some doping dependent critical temperature. The data for these films fit a heterogeneous model of conductivity, combining fluctuation induced tunnelling with metallic conductivity. Calculations of the mobility of the charge carriers in the films of various doping levels reflects the transition between the two forms of conductive behaviour. The films with a doping level of 60% have been found to exhibit the highest room-temperature conductivity, and metallic behaviour down to the lowest temperatures.

Acknowledgments

References

[1] Salaneck W R, Clark D T and Samuelsen E J (ed) 1991 *Science and Applications of Conducting Polymers* (Bristol: Hilger)
[2] Epstein A J and MacDiarmid A G 1995 *Synth. Met.* **69** 179
[3] Monkman A P and Adams P N 1991 *Synth. Met.* **41–43** 627
[4] Cao Y, Smith P and Heeger A J 1992 *Synth. Met.* **48** 91

[5]   Menon R, Yoon C O, Moses D and Heeger A J 1993 *Phys. Rev.* B **48** 17 685
[6]   Joo J, Oh E J, Min G, MacDiarmid A G and Epstein A J 1995 *Synth. Met.* **69** 251
[7]   Chiang J C and MacDiarmid A G 1986 *Synth. Met.* **13** 193
[8]   MacDiarmid A G, Chiang J C, Richter A F and Epstein A J 1987 *Synth. Met.* **18** 285
[9]   Adams P N, Laughlin P J, Monkman A P and Kenwright A M *Polymer* at press
[10] Lee K , Heeger A J and Cao Y 1993 *Phys. Rev.* B **48** 14 884
[11] Jeong S K, Suh J S, Oh E J, Park Y W, Kim C Y and MacDiarmid A G 1995 *Synth. Met.* **69** 171
[12] Park Y W, Lee Y S, Park C, Shacklette L W and Boughman R H 1987 *Solid State Commun.* **63** 1063
[13] Zuo F, Angelopolous M, MacDiarmid A G and Epstein A J 1987 *Phys. Rev.* B **36** 3475
[14] Larkin A I and Khmel'nitskii D E 1982 *Sov. Phys.–JETP* **56** 647
[15] Mott N F and Davis E A 1979 *Electronic Processes in Non Crystalline Materials* (Oxford: Clarendon)
[16] Pouget J P *et al* 1994 *Synth. Met.* **65** 131
[17] Pouget J P, Hsu C H, MacDiarmid A G and Epstein A J 1995 *Synth. Met.* **69** 119
[18] Cao Y, Smith P and Yang C 1995 *Synth. Met.* **69** 191
[19] Abell L, Adams P N, Pomfret S J and Monkman A P to be published